

Fall 12-20-2016

Auditory fatigue model applications to predict noise induced hearing loss in human and chinchilla

Pengfei Sun

Southern Illinois University Carbondale

Daniel Fox

Southern Illinois University School of Medicine

Kathleen Campbell

Southern Illinois University Springfield

Jun Qin

Southern Illinois University Carbondale, jqin@siu.edu

Follow this and additional works at: http://opensiuc.lib.siu.edu/ece_articles

Recommended Citation

Sun, Pengfei, Fox, Daniel, Campbell, Kathleen and Qin, Jun. "Auditory fatigue model applications to predict noise induced hearing loss in human and chinchilla." *Applied Acoustics* 119, No. C (Fall 2016): 57-65. doi:10.1016/j.apacoust.2016.12.007.

This Article is brought to you for free and open access by the Department of Electrical and Computer Engineering at OpenSIUC. It has been accepted for inclusion in Articles by an authorized administrator of OpenSIUC. For more information, please contact opensiuc@lib.siu.edu.

Auditory Fatigue Model Applications to Predict Noise Induced Hearing Loss in Human and Chinchilla

Pengfei Sun^a, Daniel Fox^b, Kathleen Campbell^b, Jun Qin^{a,*}

^a*Department of Electrical and Computer Engineering, Southern Illinois University, Carbondale, Illinois, USA 62901*

^b*Department of Medical Microbiology, Immunology, and Cell Biology, School of Medicine, Southern Illinois University, Springfield, IL, 62794.*

Abstract

Noise induced hearing loss (NIHL) remains a severe health problem worldwide. Current noise metrics and modeling have assessment limitations on gradually developing NIHL (GDNIHL). In this study, we applied a complex velocity level (CVL) auditory fatigue model to quantitatively assess the impact of basilar membrane (BM) movement on GDNIHL. The transfer functions of chinchilla and human auditory systems, including the triple-path nonlinear (TRNL) filters to simulate the inner ear responses, are applied to obtain BM velocity distribution. Chinchilla and human experimental hearing loss data are used to validate the proposed CVL model's effectiveness. The results reveal that the developed CVL model demonstrates high correlations with both chinchilla and human hearing loss data. The linear regression based correlation study indicates the proposed CVL model may accurately predict NIHL in both human and chinchilla.

Keywords: Noise induced hearing loss, auditory fatigue, hair cell loss, mammalian auditory filters

*Corresponding author

Email addresses: sunpengfei@siu.edu (Pengfei Sun), jqin@siu.edu (Jun Qin)

1. Introduction

Noise induced hearing loss (NIHL) is one of the most common occupationally related diseases worldwide. Exposure to excessive noise is the major avoidable cause of permanent hearing loss [1]. Over 500 million people are still at risk of developing NIHL globally [2]. Hearing loss lowers quality of life, impairs social interactions, causes isolation, and even causes loss of cognitive function. In terms of evolving time, NIHL can be briefly categorized into two types: acoustic trauma caused hearing loss and gradually developing NIHL (GDNIHL). Acoustic trauma often refers to a direct mechanical damage caused by short duration high intensity noise exposure (i.e., impulsive noise with peak sound pressure level (SPL) greater than 125 dB). GDNIHL is progressive deterioration of the auditory periphery when long-time exposed to noise with SPL above 85 dB [3]. Despite several factors (e.g., age, smoking, genetics, etc.) [2] may affect GDNIHL, the noise exposure is considered as the major cause of GDNIHL.

Several studies [4, 5, 6] show that NIHL can be considered as the mechanical failure of auditory system. Generally, conductive hearing loss and sensorineural hearing loss caused by noise exposure are presented as certain forms of mechanical malfunctions of auditory organs. For conductive hearing loss, concussion from explosion can lead to a disorder of middle ear, for instance, tympanic membrane perforations [7]. Sensorineural hearing loss occurs when there is damage to the cochlear receptor organ, and the pathology can be found in the neural, sensory, and supporting cells of cochlea [3]. As one type of sensorineural hearing loss, GDNIHL is caused by multiple exposures to excessive noise, in which the stapes footplate hammer against the oval window of cochlea. The repeated flexing of the BM squeezes or stretches the outer hair cell (OHC) and the inner hair cell (IHC), and eventually cause hearing loss in cochlea.

International standards and regulations have been developed to estimate NIHL [8, 9, 10]. The noise metrics in these standards and regulations are developed with either waveform based empirical strategies (e.g., peak acoustic pressure and pulse duration) or an auditory weighting based equal energy hypothesis

(EEH)(e.g., A-weighted equivalent sound pressure level, L_{Aeq}) [11, 12, 13]. Due to the lack of intrinsic study on the underlying mechanisms, these metrics are not sufficient enough to reveal the relation between the hearing loss and the noise exposure.

35 To better understand underlying mechanisms, an intuitive idea is to investigate the GDNIHL in auditory model (AM) framework. Such approach has three advantages: 1) transfer functions of AMs can vividly demonstrate the energy flow of noise; 2) AMs provide accurate evaluations on the ear's response to noise; 3) AMs can quantitatively describe the physical movements of hearing
40 organs (e.g., vibrations of basilar member (BM)), which is strongly correlated with GDNIHL. In recent years, AMs has been used to develop more advanced models for the assessment and prediction of NIHL. Price proposed an auditory hazard assessment algorithm for human (AHA AH) model [14] to investigate acoustic trauma caused by high-level impulse noise ($SPL \geq 140dB$). In another
45 study, Song introduced stapes velocity as an indication to predict impulse noise induced hearing loss incorporating an analog AM [15]. His model used the velocity of the stapes in the middle ear as input loads but did not involve with the auditory fatigue theory to predict of hearing loss.

For NIHL study, the key consideration for choosing an AM is how to accurately
50 quantify the flow of acoustic energy from the environment into the inner ear. As a cascade filter model, triple-path nonlinear (TRNL) filter is an efficient model to simulate mammalian cochlea (e.g., human and chinchilla) [16]. TRNL filter, as the improved version of DRNL, is more flexible and accurate on describing the response of mammalian inner ear to stimulus, including both chinchilla
55 and human beings. By introducing an extra all-pass parallel filter path, TRNL can reproduce the high-frequency plateau well. Hence, in our study, TRNL filter will be introduced to simulate the transfer function of mammalian inner ear and obtain the BM velocities.

AM is useful to describe the motions of BM responding to noise stimulus,
60 but has no indication on long-term integration effects of the noise hazardous. Considering that GDNIHL is the result of long-time accumulated hazardous, it

can be approximately treated as the fatigue damage that happens to material structures [17, 18]. Therefore, to quantitatively evaluate the long-term fatigue damage of GDNIHL, a corresponding fatigue model should be developed. The
65 fundamental principle of fatigue models is based on material fatigue theories, including the S-N curve and the Miners rule. In S-N curve scenario, the complex loads on BM are treated as the a series of sinusoidal stresses, and each adjacent load counts to the functional failure independently. Therefore, the inputs on BM are classified based on their amplitude only. Comparatively, in Miner’s
70 rule, both amplitude and median value of the stimulus are taken into accounts . Instead of using BM displacement as the inputs [19], the BM velocity is translated as complex loads against the organ of Corti [20]. The rationality lies that BM velocity not only reflects the acoustic power flowing into the inner ear, but is also highly correlated with strain and loads [21, 22].

75 In this study, we expand our previous study [23, 24] by applying our developed complex velocity level (CVL) fatigue model to predict GDNIHL in both human and chinchilla. The generalized mammalian AM incorporating the triple-path nonlinear (TRNL) filter has been used to obtain BM velocities at different cochlea partitions (i.e., Equivalent Rectangular Band (ERB)). This generalized
80 AM is adaptive to illustrate the auditory transfer functions of chinchilla and human by applying different parameters. Chinchilla and human experimental hearing loss data are applied to validate the proposed fatigue metric L_{CVL} for the prediction of GDNIHL. The preferment of the proposed model is also compared to conventional noise metrics (e.g., L_{Aeq} and L_{eq}).

85 **2. Methods AND Materials**

2.1. Transfer Functions of mammalian Auditory System

Mammalian ear comprises external, middle, and inner ears. The coupled motion of tympanic membrane (TM), ossicles, and stapes footplate are the primary path for conducting environmental sound into the inner ear.

90 *2.1.1. External ear and middle ear*

The primary function of the external ear and middle ear is to gather and conduct sound energy into the inner ear. The external ear likes a tube, with one end close by the tympanic membrane. The resonant characteristics of the external ear help determine the acoustic energy delivered to the cochlea. The middle ear acts as an impedance-matching device that compensate the transmission loss when sound is introduced to the fluid-filled cochlea [25]. The phenomenon of middle ear muscle contraction (MEMC), known as an autonomic reflex that tightens the muscles of the middle ear, can affect the transfer function of middle ear [26]. MEMC is more frequently found in impulse or impact noise circumstances [3, 27]. For generalized auditory system analysis in ambient noise, a fixed transfer function of middle ear should be used [28].

Figure.1 shows the transfer function of the external and middle ears of chinchilla [29] and human [30]. In the external ear (Fig.1a), the transfer function of human is slightly shifted from that of chinchilla and the two transfer function shapes are almost the same. In the middle ear (Fig.1b), the human transfer function is different from chinchilla. The human has significantly higher gain than the chinchilla in middle frequency range (500-5000 Hz).

In this study, transfer function of the middle ear is characterized by stapes velocity transfer function (SVTF). The SVTF was defined as the ratio between linear velocity of stapes V_S and sound pressure near the TM in the ear canal P_{TM} ($SVTF = V_S/P_{TM}$) [25], where the linear velocity V_S could be obtained by dividing volume velocity U_S by the average footplate area.

2.1.2. Inner ear model-TRNL filter

The cochlea is assumed to be a two-chambered, fluid-filled box with rigid side walls[19], and the partition between chambers is assumed rigid, excepting the flexible BM with elastic deformation. When the stapes motion produces pressure within the cochlea vestibule, sound stimulus can be transferred as BM vibrations [33]. Several phenomenological models have been introduced to simulate movements over different sites along BM [32, 34].

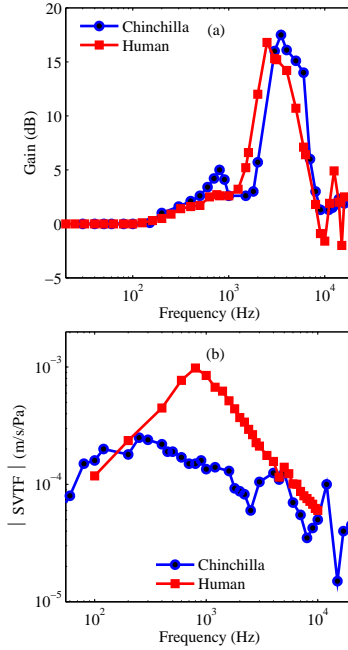


Figure 1: The transfer function of (a) the external ear and (b) the middle ear of chinchilla (blue) [31] and human (red) [32].

120 In this study, the TRNL filter [16] is utilized to obtain the BM responses along mammalian cochlea partitions. The input for TRNL filter is the linear velocity of stapes V_S and the output represents the BM velocity of a particular location along the cochlea partition. Each individual site is represented as a tuned system with three parallel signal-processes paths[32].

125 Each individual bandpass function is a cascade of two or more gammatone filters [35] with unit gain at center frequency (CF). The low pass function comprises second-order low pass filters. In the nonlinear path, the CFs and bandwidths of the gammatone filters are the same. The compressive function shape in the nonlinear path is determined from animal data, and defined as

$$y[t] = \text{SIGN}(x[t]) \times \text{MIN}(a |x[t]|, b |x[t]|^c) \quad (1)$$

130 where $x(t)$ is the output of the first filter in the nonlinear path. a , b , and c are parameters of the model. The parameter values in TRNL [32, 16] are

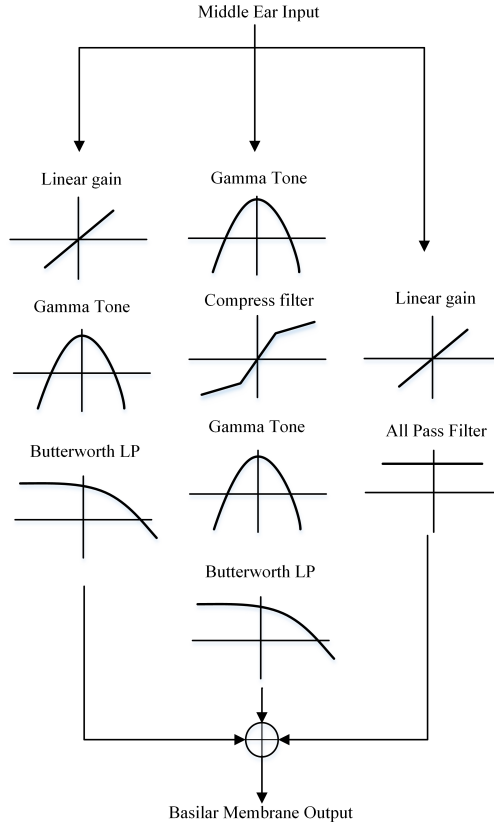


Figure 2: Schematic diagram of the TRNL filter, in which the velocities of stapes in middle ear are passed through three parallel branches to obtain the velocities of BM.

summarized in Table 1.

2.2. Basilar Membrane Velocity Based Fatigue Model CVL

In our previous work [23], complex velocity level (CVL) based on the Miner's
 135 rule was proposed to calculate noise induced cumulative hazard. Miner's rule has
 been commonly used to predict materials high-cycle fatigue life under complex
 loads. Accordingly, the CVL model takes into account potential hearing loss
 correlated with both the amplitude transition and mean value of BM velocities.
 In a single BM vibration cycle, the instantaneous hearing fatigue in Δt can be

Table 1: Parameters of the TRNL filter which are used to simulate chinchilla [16] and human inner ear [32].

	Chinchilla							Human					
	0.8kHz	5.5kHz	7.25kHz	9.75kHz	10kHz	12kHz	14kHz	0.25kHz	0.5kHz	1kHz	2kHz	4kHz	8kHz
Linear													
GT cascade	5	5	5	5	5	5	5	2	2	2	2	2	2
LP cascade	7	7	7	7	7	7	7	4	4	4	4	4	4
CF _{lin}	750	5000	7400	9000	9000	11000	13000	235	460	945	1895	3900	7450
BW _{lin}	450	3000	2500	3000	3500	5000	4000	115	150	240	390	620	1550
LP _{lin}	750	6000	7400	9000	8800	12000	13500	235	460	945	1895	3900	7450
Gain,g	500	190	3000	300	500	500	350	1400	800	520	400	270	250
Nonlinear													
GT cascade	3	3	3	3	3	3	3	3	3	3	3	3	3
LP cascade	4	4	4	4	4	4	4	3	3	3	3	3	3
CF _{lin}	730	5850	7800	9800	10000	12000	15000	250	500	1000	2000	4000	8000
BW _{lin}	350	1800	2275	1650	1800	2000	3200	84	103	175	300	560	1100
LP _{nl}	730	5850	7800	9800	10000	12000	15000	250	500	1000	2000	4000	8000
Gain,a	850	3000	15000	9000	15000	22500	3000	2124	4609	4598	9244	30274	76354
Gain,b	0.03	0.04	0.06	0.05	0.06	0.07	0.045	0.45	0.28	0.13	0.078	0.060	0.035
Exponent,c	0.25	0.25	0.25	0.25	0.25	0.25	0.25	0.25	0.25	0.25	0.25	0.25	0.25
Linear all-pass													
Gain, k	10	0.4	20	1	2	20	20	-	-	-	-	-	-

140 quantitatively described by [23]

$$\begin{aligned}
 H_{V(t),\Delta t} &= \frac{\int_{\Delta t} V(t) dN(t)}{H_0} \\
 &= \frac{\sum_j |V_j| \cdot N_j}{H_0}
 \end{aligned} \tag{2}$$

where the BM velocities $V(t)$ are regarded as complex stress, and $N(t)$ is the corresponding failure cycles at time t , respectively. In the discrete form, the subindex refers to j th category of loads. H_0 is the hearing loss at the ERB with 1 kHz CF.

145 In practice, occupational noise should be considered as complex and often random loads. Thus, the response BM velocities also demonstrate complex distribution. In the CVL model, the 2-dimensional histogram of input loads (i.e., the velocities of BM) (Fig.3a) is obtained in terms of differential velocity $V_{Amplitude}$ and mean velocity V_{mean} in the time domain (Fig.3(b))[23]. Based
150 on the histogram of complex input loads, respecting to both $V_{Amplitude}$ and V_{mean} values, the hearing loss $H_{i,CVL}$ is the integration of different categories

of inputs along the time axis as

$$H_{i,CVL} = \sum_{j \in K} N_j \cdot |V_{amplitude}(i,j) \cdot V_{mean}(i,j)| \quad (3)$$

where K is the total number of load categories, including j th type velocity, and i is the ERB band.

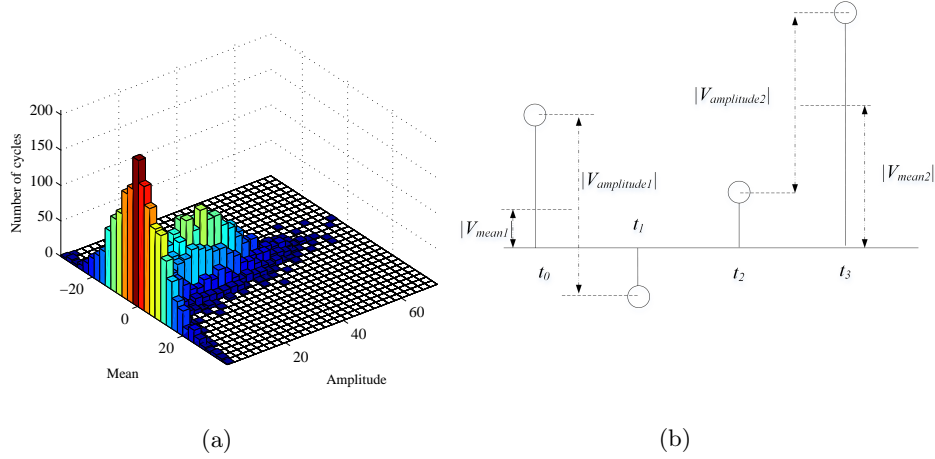


Figure 3: Histogram of BM velocities (a) categorized according to the transition amplitude and mean values of velocities as (b) at the i th ERB in 1 second.

155 Based on the i th ERB hearing loss $H_{i,CVL}$, CVL in frequency band I can be obtained

$$L_{i,CVL} = 10 \log_{10} \left(\frac{H_{i,CVL}^2}{H_0^2} \right) \quad (4)$$

$$L_{I,CVL} = 10 \log_{10} \left(\frac{\sum_{i \in I} H_{i,CVL}^2}{H_0^2} \right) \quad (5)$$

160 where $L_{i,CVL}$ and $L_{I,CVL}$ are the log scale hearing loss metrics at i th ERB and I th frequency band. $L_{i,CVL}$ reflects the integration of hearing loss level at the i th ERB temporally. Comparatively, $L_{I,CVL}$ is the hearing loss level in frequency band I , in which several ERBs might be included. Based on the CVL model, (4) and (5) can be used to assess the auditory risk of hazardous caused by the BM vibration.

2.3. Experimental Data

165 In this study, two types of hearing loss data, including chinchilla noise exposure data in the lab and human hearing loss data measured in the fields, were provided by a research group at State University of New York at Plattsburgh. The chinchilla data were used in published animal noise exposure experiments [36, 37]. The human hearing loss data were also published in recent works
170 [38, 39].

2.3.1. Chinchilla noise exposure data

Chinchilla noise exposure data were used for validation of the proposed fatigue metric. Two hundred seventy three chinchilla in 22 groups were exposed to certain noise types for five-consecutive-days at 24 hours per day. chinchilla
175 were then allowed to recover for 30 days. The 22 designed noise samples include 3 Gaussian noises with 90, 95, and 100 dBA, and 19 complex noises (one at 95 dBA, two at 90 dBA, and 16 at 100 dBA)[36, 37]. The digitally recorded noise samples (320 sec for each noise sample)[40] are used for noise analysis in this study. Detailed descriptions of the noise data and experimental protocols
180 of animal studies are available in previous publications [36, 37].

In the animal noise exposure experiments, both permanent threshold shift (PTS) and temporary threshold shift (TTS) were determined at 0.5, 1, 2, 4, 8, and 16 kHz for each animal as summarized in Table 2. In addition, to assess the overall hearing loss in whole frequency range, the averaged effective PTS has
185 been proposed as $PTS_{1248} = \frac{1}{4}(PTS_1 + PTS_2 + PTS_4 + PTS_8)$, where PTS_1 , PTS_2 , PTS_4 , and PTS_8 are the PTS value measured at the octave band with center frequency 1, 2, 4, and 8 kHz, respectively. The same rule was applied to TTS to obtain TTS_{1248} .

190 2.3.2. Human hearing loss data

The human hearing loss data comprised Gaussian and non-Gaussian industrial noise recordings and hearing levels from workers in two noisy industrial

Table 2: PTS and TTS of Chinchilla at different center frequencies of octave bands for different noise exposures.

Samples	L_{Aeq}	PTS						TTS					
		0.5 kHz	1 kHz	2 kHz	4 kHz	8 kHz	16 kHz	0.5 kHz	1 kHz	2 kHz	4 kHz	8 kHz	16 kHz
G44	100.6	17.1	26.2	39.4	42.9	46.5	43.7	58.6	70.1	79.3	85.4	85.8	70.6
G49	101	22.1	34.3	47.2	54.6	46.8	47.2	62.6	75.3	77.6	86.5	79.9	70.6
G50	100.5	7.7	10.1	8.0	15.8	14.1	17.7	37.2	57.6	63.4	76.1	79.8	69.2
G51	100.1	15.7	19.5	29.0	24.3	27.8	25.1	59.7	63.9	73.2	75.9	81.9	67.9
G52	101.7	18.5	24.5	36.8	32.9	28.3	23.3	63.9	72.4	76.4	81.2	80.1	69.6
G53	100.6	19.0	24.4	34.5	31.7	29.9	28.1	59.4	68.0	77.4	85.0	84.3	69.0
G54	100.6	16.2	18.5	29.9	31.4	25.4	29.1	55.7	65.3	75.6	82.5	80.0	66.3
G55	100.1	18.8	21.7	36.5	46.8	60.1	47.5	67.1	74.1	76.2	82.3	80.3	68.8
G60	100.2	20.7	27.8	34.1	34.1	29.3	27.8	59.3	68.4	70.8	75.7	75.9	65.2
G61	99.6	2.6	5.0	10.0	20.5	18.2	24.0	36.1	45.6	50.4	74.4	80.4	72.0
G63	99.6	25.4	31.4	43.8	36.2	32.3	28.9	63.4	69.8	76.2	76.4	73.4	65.0
G64	101.1	15.8	17.4	24.7	22.1	19.0	13.5	60.0	66.3	73.8	79.4	73.9	67.1
G65	99.7	17.2	14.4	25.0	39.6	49.5	48.3	62.5	62.8	68.1	74.4	75.8	70.7
G66	100.7	7.5	9.3	19.2	32.9	44.8	36.2	49.4	58.9	70.0	82.9	76.1	70.4
G68	99.7	12.9	13.9	21.7	39.7	47.3	47.3	65.9	69.2	71.1	81.1	75.0	73.3
G69	101	4.8	10.9	9.3	11.3	5.5	8.0	28.8	47.4	48.8	49.3	47.8	50.1
G70	100.7	12.1	17.9	27.6	43.2	30.4	35.1	59.9	69.9	75.0	84.8	76.8	71.0
G47	89.4	0.3	-0.3	3.6	1.5	7.9	7.0	22.5	35.0	43.3	60.8	68.7	61.2
G48	91.7	3.0	6.8	9.4	5.4	11.2	10.8	26.9	35.9	37.6	41.5	58.0	63.9
G56	91.3	2.9	1.7	4.5	8.9	14.7	8.9	29.5	30.5	29.2	39.3	52.0	50.9
G57	94.2	6.8	5.8	6.7	16.7	23.3	18.9	35.5	41.4	52.1	66.4	71.8	66.0
G58	95.6	7.8	8.8	18.9	17.5	15.0	17.9	44.5	50.3	59.1	62.1	62.1	63.6

environments [38, 39]. All participants were required to satisfy the following four criteria: (1) a minimum of at least 1-yr employment at the current task, (2) no history of genetic or drug-related hearing loss, head trauma, or ear diseases, (3) no military service, shooting activities, or high intensity nonindustrial noise exposure, and (4) no history of hearing protection use. A total of 195 workers out of 220 participants from two industries met the study criteria. Thirty-two of the participants were exposed to non-Gaussian noise for an average of 12.3 ± 7.1 yrs in a metal fabrication factory. The remaining 163 participants were exposed to a continuous Gaussian noise for an average 12.7 ± 8.4 yrs in a textile mill.

Each enrolled participant was given a general physical and an otologic examination. Pure air tone, conduction hearing threshold levels (HTLs) at 0.5, 1.0, 2.0, 3.0, 4.0, 6.0, and 8.0 kHz were measured by an experienced physician for right and left ears. HTLs at each frequency were adjusted for age and gender using the 50th percentile values found in the standard [8] Annex B. Real-time noise signals (5-min duration) were recorded at the level of the participants ear. Nineteen noise signals from the non-Gaussian noise environment and 20 from the Gaussian noise environment were recorded with 16-bit resolution and 11

210 kHz sampling rate. Among these samples, 14 noises, ranging from 90 dBA to 105 dBA were used for noise analysis in this study (Table 3). The Nyquist limit (5.5 kHz) limited PTS analysis to no more than a frequency band centered at 6 kHz. As a result, the 8 kHz PTS data is not presented in Table 3. In this study, the PTS collected at frequency band with 6 kHz CF has been processed
 215 by a linear approximation to obtain the PTS at the frequency band with 5 kHz CF. In addition, the averaged PTS, including PTS_{1234} and PTS_{2345} are used to evaluate the overall NIHL.

Table 3: PTS loss of Human at different frequency bands for different noise exposures.

Samples	L_{Aeq}	Right Ear						Left Ear					
		0.5 kHz	1 kHz	2 kHz	3 kHz	4 kHz	6 kHz	0.5 kHz	1 kHz	2 kHz	3 kHz	4 kHz	6 kHz
Gm5c1a	98.7	14.3	11.8	16.1	28.5	32.5	24.8	17.3	13.8	12.1	28	33	26.3
Gm5c1b	96.1	14.1	12.2	12.2	19.3	19.5	16.2	12.9	11.8	10.7	12	15.2	19.6
Gm5c2a	95	13.6	13.6	12.2	9.9	14.8	17.7	16.1	13.6	11.2	9.9	14.8	12.2
Gm5c2b	104.5	16.5	17.1	13.4	15.5	16.4	16.5	15.3	14	12.8	16.8	16.4	16.5
Gm5c3a	103	16.3	16.3	21.4	27	23.3	26.4	16.3	12.7	13.6	22.7	23.3	30
Gm5c3b	100.6	15.3	16.7	23.7	32.9	34.1	42.7	15.3	13.9	18.7	32.9	32	29.1
Gm5c4a	95.5	14.4	17.9	16.1	28.2	31.4	35.6	15.8	15.8	16.1	24.3	30.3	25.9
Gm5c4b	105.6	15.1	15.1	16.2	32.9	40.3	36.7	16.3	13.8	14.9	27.1	40.7	37.1
Gm5c5a	97	10.4	10.4	9	14.3	13.7	10.9	13.3	10.4	8.3	7.9	13.7	15.1
Gm5c5b	100.3	12.1	12.5	19.7	25.1	30.7	30	16.6	13.5	19.7	26.5	34.8	31.4
Gm5c6a	92	18.7	17.3	25.7	38.7	43	40.7	18	15.1	18.6	30.1	35.1	43.6
Gm5c8a	101.1	13.6	12.3	9.2	11.3	17.4	19.9	13.6	12.1	8.0	12.3	21.9	21.7
Tcc1a	92.1	15.2	13	11.6	23.4	34.4	35.3	16.9	14.7	12.7	24	38.9	28.7
Tcc6a	95.2	12.9	10.4	9.9	12.9	12.9	17.6	11	10.4	8	12.3	11.6	18.9

3. RESULTS AND DISCUSSIONS

220 3.1. BM Velocity Distributions Obtained by the Chinchilla and Human Auditory Models

Four experimental noise samples (i.e., G63 and G61 from chinchilla, and Tcc1a and Gm5c2a from human) were used as inputs to test the AMs of chinchilla and human. The time-frequency (T-F) presentation of the BM velocity distributions are shown in Fig.4. The noise sample G63 simulates an impulsive noise (Fig.4(a)), while the sample G61 is a typical Gaussian continuous noise (Fig.4(b)). The recorded metal fabrication factory noise sample Tcc1a is a non-Gaussian noise (Fig.4(c)). Comparatively, the noise sample Gm5c2a (Fig.4(d))
 225 collected from textile mill is a Gaussian noise.

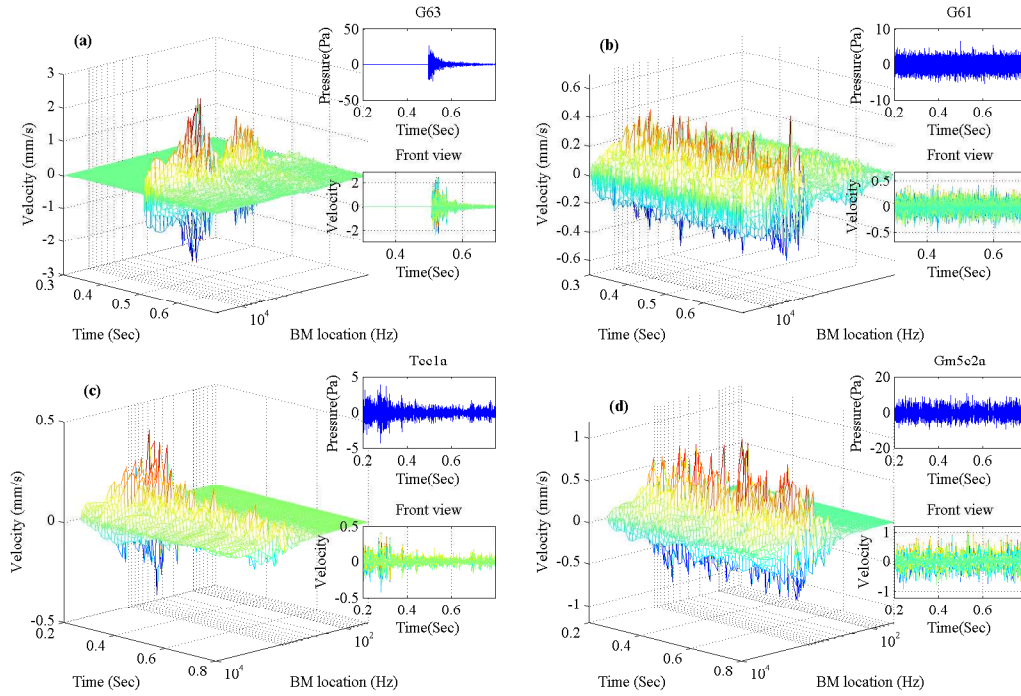


Figure 4: Time-frequency presentations of the BM velocities obtained by the developed chinchilla and human auditory models, responding to the experimental noise samples (a)G63,(b)G61, (c)Tcc1a, and (d)Gm5c2a. The partial waveforms of G63, G61, Tcc1a, and Gm5c2a in 0.6 sec are shown in the top insert figures. The front views of the distributions of the BM velocities are shown in the bottom insert figures.

230 The distributions of the BM velocities along the time axis can accurately reflect the waveform of original noise signals (Figure 4 a-d front views). The AMs accurately transfer the acoustic pressure to the BM velocities in both chinchilla and human models. Furthermore, for chinchilla, the distributions of the BM velocities along the frequency axis are concentrated in the high frequency bands (Fig.4(a),(b)). The BM velocities in the low frequency bands were significantly reduced by the chinchilla external-middle ear transfer function gain (as shown in Fig.1), which demonstrates a strong decayed gain at low frequency range. In contrast, for human (as shown in Fig.4(c) and 4(d)), the BM velocities are concentrated within frequency range of 500-5000 Hz. This is consistent with the transfer function of human middle ear (as shown in Fig.1(b)), which has significantly higher gain than the corresponding transfer function of chinchilla.

235

240

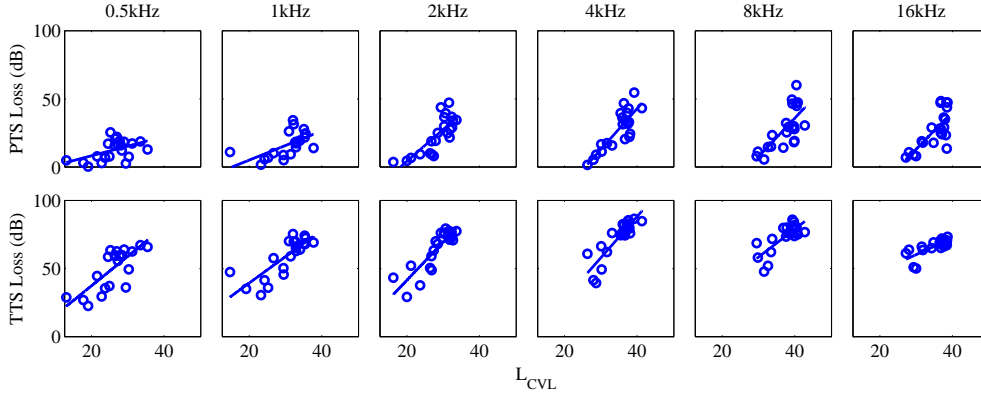


Figure 5: Scatting plots and fitting lines of pairs of the developed fatigue metrics L_{CVL} , and hearing loss indications, TTS and PTS at six octave frequency bands, averaged by all 22 groups of animal experimental data.

3.2. Validation of the Developed CVL Fatigue Models in Chinchilla

3.2.1. Linear regression analysis at six octave bands

The linear regression analysis of the developed fatigue metric (L_{CVL}), and two hearing loss indications (PTS and TTS) at six frequency bands were conducted using all 22 chinchilla noise exposure groups. Figure 5 shows the fitting lines and scatting plots of the pairs of L_{CVL} and the hearing loss indices. L_{CVL} is calculated using a 40-sec time window. Each symbol in Fig.5 refers to a pair of a fatigue metric and an animal hearing loss index. The lines indicate the fitting results of the distributions of symbols. Six octave frequency bands centered at 0.5, 1, 2, 4, 8, and 16 kHz cover the BM frequency range.

Moreover, the linear correlation value (r^2) of different metrics, including L_{Aeq} , L_{eq} and the proposed L_{CVL} , showed that in each octave frequency band, L_{CVL} achieves the higher correlation with both PTS and TTS compared to the two conventional L_{Aeq} and L_{eq} metrics (Table 4). L_{CVL} has strong correlations with hearing loss indices at frequency bands centered at 1, 2, 4, and 8 kHz than 0.5 and 16 kHz because with higher r^2 values. In addition, L_{CVL} showed the higher correlations with TTS than PTS at all frequency bands. TTS refers to the instant hearing loss immediately after a noise exposure, while the PTS is the permanent hearing loss after noise exposure with certain recovery time [6]. TTS

directly reflects the mechanical failure caused by noise exposure. The developed fatigue models are based on the BM velocity, which reflects the mechanical vibration of BM in cochlea. Therefore, it is reasonable that the proposed fatigue metrics have higher correlations with TTS.

Table 4: Regression analysis of two hearing loss indices of chinchilla and different metrics at six octave bands centered at 0.5, 1, 2, 4, 8, and 16 kHz

r^2	0.5kHz	1kHz	2kHz	4kHz	8kHz	16kHz
L_{CVL} -PTS	0.25	0.41	0.77	0.71	0.52	0.55
L_{Aeq} -PTS	0.09	0.39	0.25	0.53	0.32	0.15
L_{eq} -PTS	0.07	0.37	0.25	0.54	0.30	0.12
L_{CVL} -TTS	0.57	0.65	0.81	0.76	0.65	0.57
L_{Aeq} -TTS	0.29	0.57	0.41	0.60	0.50	0.51
L_{eq} -TTS	0.27	0.54	0.40	0.61	0.52	0.49

265 *3.2.2. Linear regression analysis based on overall hearing loss*

Overall hearing loss indices averaged by the octave bands centered at 1, 2, 4, and 8 kHz, including TTS_{1248} , and PTS_{1248} , were used in a regression analysis to further evaluate the effectiveness of the proposed fatigue metric on NIHL prediction. The scattng plots and the fitting lines of the pairs of the developed
 270 fatigue metrics and TTS_{1248} and PTS_{1248} are shown in Fig.6. L_{CVL} achieved high r^2 values with both TTS_{1248} and PTS_{1248} . Thus, the developed fatigue metric correlates well the chinchilla experimental hearing loss. Compared to PTS_{1248} , L_{CVL} also has a higher correlation with TTS_{1248} .

Table 5 demonstrates L_{CVL} 's advantage over conventional noise metrics
 275 (e.g., L_{Aeq} and L_{eq}). The r^2 value comparisons of the three metrics with respect to TTS_{1248} and PTS_{1248} show significantly higher correlations between L_{CVL} and both hearing loss indications compared to L_{Aeq} and L_{eq} . Thus, the considerably high correlations between the L_{CVL} and hearing loss data suggests that the proposed CVL model may accurately predict GDNIHL in chinchilla.

280 *3.3. Validation of CVL Models in Human*

The same procedure was implemented to conduct the linear regression analysis of L_{CVL} and PTS at six frequency bands centered at 0.5, 1, 2, 3, 4, and 5

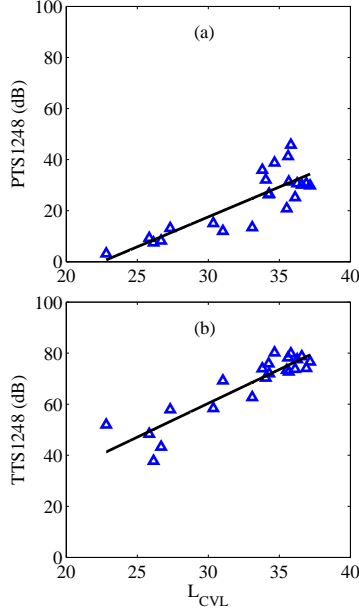


Figure 6: Regression analysis of averaged PTS_{1248} and TTS_{1248} of chinchilla and proposed fatigue metric L_{CVL} with R^2 value 0.7 (a) and 0.82 (b), respectively.

Table 5: Regression analysis of two hearing loss indices of chinchilla and different metrics at averaged octave bands

	PTS_{1248}	TTS_{1248}
L_{CVL}	0.7	0.82
L_{Aeq}	0.48	0.62
L_{eq}	0.47	0.59

kHz with 195 human participants.

In Fig.7, the horizontal coordinates of the 14 dots represent the L_{CVL} of 14
 285 occupational noise samples in each frequency band, whereas the vertical coordi-
 nates of the 14 dots in each sub-figure reflects the averaged PTS of participants
 exposed to certain noise samples. L_{CVL} has a strong correlation with PTS in
 the 2, 3, 4, and 5 kHz frequency bands. L_{CVL} is also linearly correlated with
 the PTS in all the frequency bands and peaks at 0.72 in the 5 kHz frequency
 290 band (Table 6). In addition, L_{CVL} has significantly higher r^2 values in all six
 frequency bands compared to L_{Aeq} and L_{eq} . Results indicate the L_{CVL} metric

Table 6: Regression analysis of PTS of human and different metrics at six frequency bands centered at 0.5, 1, 2, 3, 4, and 5 kHz

r^2	0.5kHz	1kHz	2kHz	3kHz	4kHz	5kHz
$L_{CVL} - PTS$	0.38	0.40	0.62	0.59	0.68	0.72
$L_{Aeq} - PTS$	0.08	0.13	0.51	0.44	0.42	0.32
$L_{eq} - PTS$	0.09	0.11	0.49	0.47	0.41	0.30

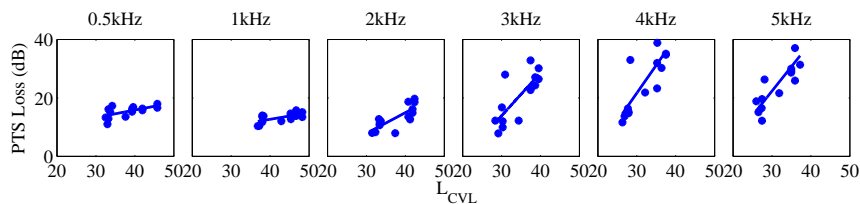


Figure 7: Scatting plots and fitting lines of pairs of the developed fatigue metric, L_{CVL} , and hearing loss indication (i.e., PTS) at six frequency bands, averaged by all of human hearing loss data in each group.

may be able to more accurately predict NIHL than conventional noise metrics, e.g., L_{Aeq} and L_{eq} .

Moreover, two averaged hearing loss indices PTS_{1234} and PTS_{2345} were used to validate the effectiveness of L_{CVL} in the prediction of overall hearing loss in human. L_{CVL} is linearly correlated with human hearing loss data (Fig.8) and the metric L_{CVL} measured higher r^2 values than both L_{Aeq} and L_{eq} (Table 7). Results indicate the proposed CVL model may accurately predict the GDNHL caused by occupational noise (including both Gaussian an non-Gaussian noise) in human.

Table 7: Regression analysis of two hearing loss indices (PTS_{1234} and PTS_{2345}) of human and different metrics at averaged octave bands

	PTS_{1234}	TTS_{2345}
L_{CVL}	0.7	0.74
L_{Aeq}	0.56	0.57
L_{eq}	0.54	0.49

The hearing damage calculated by the proposed auditory fatigue model accu-

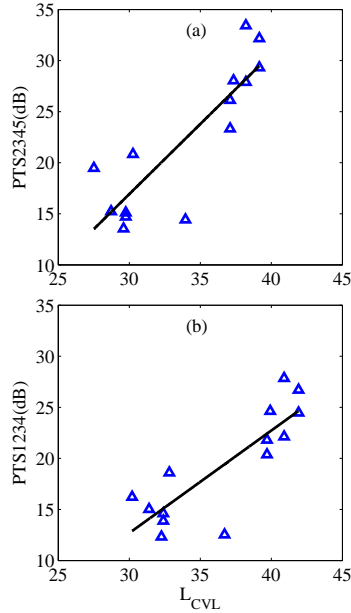


Figure 8: Scatting plots and fitting lines of (a) L_{CVL} vs. PTS_{2345} and (b) L_{CVL} vs. PTS_{1234} averaged by all each group of human hearing loss data.

rately fits the hearing loss data for both chinchilla and human. It strengthens the conclusion that the hearing loss is a reflection of auditory fatigue phenomenon. In addition, the chinchilla has been the most common animal model for noise induced hearing loss (NIHL) in human with 221 articles published since 1971 [41].
 305 Regardless of the study target tissue in the various studies, the noise exposure must first pass through the cochlea. Thus the information in this study may indicate that the commonly used chinchilla model is appropriate to translate research in NIHL to human.

310 4. Conclusion

In this study, an auditory fatigue model (i.e., CVL model) was tested as a predictor of occupational noise-induced GDNIHL for both chinchilla and human. The mammalian AM was introduced by combining the TRNL filter with external-middle ear transfer function to accurately characterize BM vibration.

315 Both animal noise exposure data and human field hearing loss data were used
to validate the effectiveness of the developed CVL model. Results indicated
the developed CVL model demonstrated high correlations with experimental
hearing loss data in both chinchilla and human. The proposed metric L_{CVL}
also showed significant advantage on hearing loss prediction compared to L_{Aeq}
320 and L_{eq} . Results indicate that the developed model may accurately predict the
NIHL in both chinchilla and human. The developed CVL model may be applied
for human NIHL assessment in various industrial and military applications.

Acknowledgment

This research was supported in part by National Institute on Deafness and
325 Other Communication Disorders (NIDCD)(R01 DC014549-01), and Illinois Clean
Coal Institute with funds made available by the State of Illinois. The authors
thank Wei Qiu at the State University of New York at Pittsburgh for providing
chinchilla noise exposure and human hearing loss data.

References

- 330 [1] Y. Agrawal, E. A. Platz, J. K. Niparko, Prevalence of hearing loss and differences by demographic characteristics among us adults: data from the national health and nutrition examination survey, 1999-2004, *Archives of Internal Medicine* 168 (14) (2008) 1522–1530.
- [2] M. Sliwinska-Kowalska, A. Davis, et al., Noise-induced hearing loss, *Noise and Health* 14 (61) (2012) 274.
- 335 [3] D. Henderson, R. P. Hamernik, Biologic bases of noise-induced hearing loss, *Occupational Medicine-State of the Art Reviews* 10 (3) (1995) 513–534.
- [4] H. Crane, Mechanical impact: a model for auditory excitation and fatigue, *The Journal of the Acoustical Society of America* 40 (5) (1966) 1147–1159.
- 340 [5] G. R. Bock, E. J. Seifter, Developmental changes of susceptibility to auditory fatigue in young hamsters, *International Journal of Audiology* 17 (3) (1978) 193–203.
- [6] B. C. J. Moore, *An introduction to the psychology of hearing*, Brill, 2012.
- [7] J. C. Steinberg, M. B. Gardner, The dependence of hearing impairment on sound intensity, *The Journal of the Acoustical Society of America* 9 (1) 345 (1937) 11–23.
- [8] *Acoustics – estimation of noise-induced hearing loss*, Standard, International Organization for Standardization, Geneva, CH (Oct. 2013).
- [9] U. D. of Health, H. Services, et al., *Criteria for a recommended standard: occupational noise exposure. revised criteria 1998*, Centers for Disease Control and Prevention, National Institute for Occupational Safety and Health.
- 350 [10] U. D. of Defense, *Department of defense design criteria standard: Noise limits (mil-std-1474d)*.

- [11] M. H. Azizi, Occupational noise-induced hearing loss, *The international journal of occupational and environmental medicine* 1 (3 July).
355
- [12] W. J. Murphy, C. A. Kardous, A case for using a-weighted equivalent energy as a damage risk criterion, National Institute for Occupational Safety and Health, EPHB Report No.
- [13] P. Sun, J. Qin, W. Qiu, Development and validation of a new adaptive weighting for auditory risk assessment of complex noise, *Applied Acoustics* 103 (2016) 30–36.
360
- [14] G. R. Price, Predicting mechanical damage to the organ of corti, *Hearing research* 226 (1) (2007) 5–13.
- [15] W. J. Song, Study on human auditory system models and risk assessment of noise induced hearing loss, University of Cincinnati, 2010.
365
- [16] A. Lopez-Najera, R. Meddis, E. A. Lopez-Poveda, A computational algorithm for computing cochlear frequency selectivity: Further studies, in: *Auditory Signal Processing*, Springer, 2005, pp. 14–20.
- [17] N. Slepecky, Overview of mechanical damage to the inner ear: noise as a tool to probe cochlear function, *Hearing research* 22 (1) (1986) 307–321.
370
- [18] B. Hu, Noise-induced structural damage to the cochlea, in: *Noise-Induced Hearing Loss*, Springer, 2012, pp. 57–86.
- [19] G. R. Price, J. T. Kalb, Insights into hazard from intense impulses from a mathematical model of the ear, *The Journal of the Acoustical Society of America* 90 (1) (1991) 219–227.
375
- [20] J. Deng, S. Chen, X. Zeng, G. Li, Using a dynamic tracking filter to extract distortion-product otoacoustic emissions evoked with swept-tone signals, *Biomedical and Health Informatics, IEEE Journal of* 18 (4) (2014) 1186–1195.

- 380 [21] M. A. Ruggero, S. S. Narayan, A. N. Temchin, A. Recio, Mechanical bases of frequency tuning and neural excitation at the base of the cochlea: comparison of basilar-membrane vibrations and auditory-nerve-fiber responses in chinchilla, *Proceedings of the National Academy of Sciences* 97 (22) (2000) 11744–11750.
- 385 [22] L. Robles, M. A. Ruggero, Mechanics of the mammalian cochlea, *Physiological reviews* 81 (3) (2001) 1305–1352.
- [23] P. Sun, J. Qin, K. Campbell, Fatigue modeling via mammalian auditory system for prediction of noise induced hearing loss, *Computational and mathematical methods in medicine* 2015.
- 390 [24] P. Sun, J. Qin, Auditory fatigue models for prediction of gradually developed noise induced hearing loss, in: *2016 IEEE-EMBS International Conference on Biomedical and Health Informatics (BHI)*, IEEE, 2016, pp. 384–387.
- [25] M. C. Slama, M. E. Ravicz, J. J. Rosowski, Middle ear function and cochlear input impedance in chinchilla, *The Journal of the Acoustical Society of America* 127 (3) (2010) 1397–1410.
- 395
- [26] M. Bance, F. M. Makki, P. Garland, W. A. Alian, R. G. Van Wijhe, J. Savage, Effects of tensor tympani muscle contraction on the middle ear and markers of a contracted muscle, *The Laryngoscope* 123 (4) (2013) 1021–1027.
- 400
- [27] W. A. Ahroon, Effects of acoustic impulses on the middle ear, Tech. rep., DTIC Document (2015).
- [28] B. Moore, B. Glasberg, A model of loudness perception applied to cochlear hearing loss, *Auditory Neuroscience* 3 (3) (1997) 289–311.
- 405 [29] P. A. Vrettakos, S. P. Dear, J. C. Saunders, Middle ear structure in the chinchilla: a quantitative study, *American journal of otolaryngology* 9 (2) (1988) 58–67.

- [30] R. L. Goode, M. Killion, K. Nakamura, S. Nishihara, New knowledge about the function of the human middle ear: development of an improved analog model., *Otology & Neurotology* 15 (2) (1994) 145–154.
- [31] J. J. Rosowski, The effects of external-and middle-ear filtering on auditory threshold and noise-induced hearing loss, *The Journal of the Acoustical Society of America* 90 (1) (1991) 124–135.
- [32] R. Meddis, L. P. OMard, E. A. Lopez-Poveda, A computational algorithm for computing nonlinear auditory frequency selectivity, *The Journal of the Acoustical Society of America* 109 (6) (2001) 2852–2861.
- [33] W. Rhode, N. Cooper, Nonlinear mechanics in the apical turn of the chinchilla cochlea in vivo, *Auditory Neuroscience* 3 (2) (1996) 101–121.
- [34] A. J. Oxenham, C. A. Shera, Estimates of human cochlear tuning at low levels using forward and simultaneous masking, *Journal of the Association for Research in Otolaryngology* 4 (4) (2003) 541–554.
- [35] W. M. Hartmann, *Signals, sound, and sensation*, Springer Science & Business Media, 1997.
- [36] R. P. Hamernik, W. Qiu, Energy-independent factors influencing noise-induced hearing loss in the chinchilla model, *The Journal of the Acoustical Society of America* 110 (6) (2001) 3163–3168.
- [37] R. P. Hamernik, W. A. Ahroon, Sound-induced priming of the chinchilla auditory system, *Hearing research* 137 (1) (1999) 127–136.
- [38] Y.-m. Zhao, W. Qiu, L. Zeng, S.-s. Chen, X.-r. Cheng, R. I. Davis, R. P. Hamernik, Application of the kurtosis statistic to the evaluation of the risk of hearing loss in workers exposed to high-level complex noise, *Ear and hearing* 31 (4) (2010) 527–532.
- [39] G. S. Goley, W. J. Song, J. H. Kim, Kurtosis corrected sound pressure level as a noise metric for risk assessment of occupational noises, *The Journal of the Acoustical Society of America* 129 (3) (2011) 1475–1481.

- [40] R. P. Hamernik, W. Qiu, B. Davis, Hearing loss from interrupted, intermittent, and time varying non-gaussian noise exposure: The applicability of the equal energy hypothesis, *The Journal of the Acoustical Society of America* 122 (4) (2007) 2245–2254.
- 440 [41] K. Campbell, A. Claussen, R. Meech, S. Verhulst, D. Fox, L. Hughes, D-methionine (d-met) significantly rescues noise-induced hearing loss: Timing studies, *Hearing research* 282 (1) (2011) 138–144.